Preprints of the 19th World Congress
The International Federation of Automatic Control
Cape Town, South Africa. August 24-29, 2014

Analysis of Errors in a High Accuracy Sampled-data Stabilising System Operating with a Wide Range of PWM

Ruslan Zarovskyi*, Roustiam Chakirov** and **Yuriy Vagapov*****

** Department of Industrial Electronics, Chernihiv State Technological University, 95 Shevchenko Street, Chernihiv, 14027, Ukraine (e-mail: rolandzar@ukr.net)*
*** Department of Electrical and Mechanical Engineering, Bonn-Rhein-Sieg University of Applied Science, 20 Grantham-Allee, Sankt Augustin, D-53757, Germany (e-mail: roustiam.chakirov@h-brs.de)*
**** Department of Engineering and Applied Physics, Glyndwr University, Plas Coch, Mold Road, Wrexham, LL11 2AW, UK (e-mail: y.vagapov@glyndwr.ac.uk)*

Abstract: This paper presents a new method of analysing the error of a sampled-data velocity stabilising system with a wide range of pulse width modulation. The analysis is based on multi-channel model obtained as a result of approximation of pulse-modulated signal at the output of a PWM converter. Approximation of piecewise-linear modulation characteristics of each channel has been obtained as a series expansion of Hermite polynomials where the expansion comprises two polynomials of the first and third orders. The transfer function of every channel and a closed-loop system has been obtained using multidimensional Z-transform. The analytical expression of an error under impact of a step input has been derived using a transfer function of the closed-loop system. A dc electric drive has been used as an example of high accuracy sample-data stabilising system to verify and demonstrate the proposed method.

Keywords: Nonlinear sampled-data system, Pulse-width modulation, Volterra-Wiener series, Multidimensional Z-transforms, dc electric drive.

1. INTRODUCTION

The performance of electromechanical systems is often characterised by the accuracy of regulation or stabilisation of output parameters such as velocity or position. The accuracy is usually estimated using analysis of a control error of the investigated system. However, the solution of the accuracy obtained analytically can be used for further optimisation of the system to make it robust to random influences. Therefore, the analytical solution is important for the design and effective turning of electromechanical systems' control.

The pulse width modulation (PWM) technique is widely applied for control in power electronic systems. Analogue components used for PWM control circuits in the past have been recently replaced by digital controllers making PWM control much simpler, cheaper and reliable. However, due to the discrete nature of digital control, the signals in such systems are processed with a delay affecting the real-time performance.

The analysis of discrete systems is often based on sampled-data theory. This theory has received much attention in recent decades due to the intensive development of digital control and there has been significant progress, particularly in the area of linear sampled-data systems. However, the increase in speed and accuracy of operations inevitably involves nonlinearity of real elements in the system analysis. The presence of nonlinear elements in a sampled-data system dramatically changes its properties.

The analysis of nonlinear systems is often based on linearisation of nonlinear systems where the original nonlinear system is replaced by an equivalent linear. Obviously, the linearised model can not fully replace a nonlinear system, but in some cases it is permissible. Therefore, well-known methods applied for analysis of linear systems can be used to study linearised models (Lang et al., 2007; Li et al., 2011; Pavlov et al., 2007). Although the linearisation methods produce solutions relatively fast, without complex mathematical calculations, the accuracy of results is usually low.

A better result can be obtained using the method of analysis based on Volterra-Wiener functional series and multidimensional Z-transform (Schetzen, 2006; Rugh, 1981). The advantage of this method is a high accuracy description of a nonlinear control object. However, for the high accuracy results the efficiency of the method might be reduced as it employs additional computational resources.

This paper presents a new method for the analysis of nonlinear systems operating with a deep PWM. This method is based on a combination of several approximations of output signal of pulse converter and its regulation characteristic with a subsequent use of multidimensional discrete Laplace transform. A control system of a dc electric drive with PWM has been chosen as an example of a high accuracy sampled-data stabilising system to demonstrate the ability of the proposed method in finding an analytical solution.

2. MODELLING METHODS

The analysis of linear automatic control systems is often performed in the frequency domain using Fourier transform. However, Fourier transform requires a significant computational resource to perform a large number of math operations such as multiplication. Walsh transform, as alternative to

Fourier, can dramatically reduce computations, particularly for signals whose waveform is similar to the shape of the base functions of a Walsh series.

The method used in this paper for function approximation is Hermite polynomials $H_n(x)$ which is orthogonal polynomials (Burden and Faires, 2011) defined as

$$H_n(x) = (-1)^n e^{x^2} \frac{d^n}{dx^n}\left(e^{-x^2}\right) \quad (1)$$

Another way to obtain these polynomials is by using the recurrence relation given below

$$H_n(x) = 2nH_{n-1}(x) \quad (2)$$

The first four Hermite polynomials are expressed as

$$\begin{gathered} H_0(x) = 1;\ H_1(x) = 2x; \\ H_2(x) = 4x^2 - 2;\ H_3(x) = 8x^3 - 12x \end{gathered} \quad (3)$$

Hermite polynomials can be used to expand various functions in series. According Burden and Faires (2011) expansion of a function $f(x)$ in series has the following form:

$$f(x) = \sum_{n=0}^{\infty} c_n H_n(x) \quad (4)$$

where c is coefficient of Hermite series; n is a serial number of coefficient. The coefficients of the series are calculated as

$$c_n = \frac{1}{\sqrt{2\pi}\sigma} \int_{-\infty}^{+\infty} e^{-\frac{x^2}{2\sigma^2}} f(x) H_n(x) dx \quad (5)$$

where $f(x)$ is an approximated function; σ is the dispersion of argument x.

Series expansion by Hermite polynomials takes into account the probability of function argument. The probability is often adopted as a random variable with normal distribution.

Z-transform is commonly used for analysis and design of linear sampled-data and discrete-continuous automatic control systems. However, Schetzen (2006) has proved that Z-transform can be applied to nonlinear systems by using the functional series of Volterra-Wiener.

The following equation describes a typical nonlinear system

$$y(t) = N\{x(t)\} \quad (6)$$

where $x(t)$ is the input signal, $y(t)$ is the output signal, $N\{\}$ is non-linear operator.

If the operator is continuous, the system can be decomposed in the functional series of Volterra-Wiener

$$y(t) = \sum_{n=1}^{\infty} y_n(t) = \sum_{n=1}^{\infty} \int_0^{\infty} \cdots \int_0^{\infty} w_n(\tau_1, \ldots, \tau_n) \prod_{i=1}^{n} x(t-\tau_i) d\tau_i \quad (7)$$

where $w_n(t_1, t_2, \ldots t_n)$ is the kernel of Volterra series with order n or n-dimensional weight function.

It can be seen from (7) that response of a nonlinear system contains a linear $y_1(t)$ and nonlinear components $y_2(t)$ $y_3(t)$,… The linear component $y_1(t)$ is obtained by convolution of the input signal $x(t)$ with a first-order Volterra kernel $w_1(t)$. The non-linear components are n-dimensional convolutions of the input signal and n-th order Volterra kernels. Then the n-th order Volterra kernel can be viewed as multidimensional weighting function of a nonlinear system. In this case, nonlinear system is completely defined by a set of equivalent transfer functions $W_n(z_1, \ldots, z_n)$ obtained by applying the multidimensional Z-transform to the terms of the functional decomposition. Multidimensional equivalent transfer functions are used to find responses of an open-loop and a closed-loop nonlinear sampled-data systems in respect of the input signal.

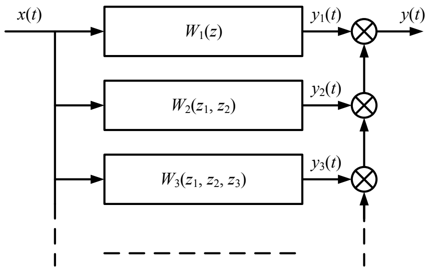

Fig. 1. Equivalent block diagram of nonlinear systems

Therefore, the model of the investigated system can be designed as parallel connection of units corresponding to the components of the functional series. It means that any nonlinear system can be represented by an equivalent block diagram shown in Fig. 1, where $W_n(z_1, \ldots, z_n)$ is the equivalent multidimensional transfer functions.

3. ANALYSIS OF ERROR

Fig. 2 shows a sampled-data single-loop automatic control system of an electric drive. The aim of the system control is to stabilise the output speed of the motor ω_{out} in respect of the input reference signal ω_{in}. The actual motor speed ω_{out} is measured and compared with the input reference signal ω_{in} to produce an error $e = \omega_{in} - \omega_{out}$. The error signal is converted by the control system block into a duty cycle γ. The PWM block generates the voltage V_{PMW} to supply a dc motor in accordance of the duty cycle γ. For this purpose, the dc motor can be described as a first-order transfer function (8).

$$W_{DCM}(s) = \frac{K_{DCM}}{T_{EM}s + 1} \quad (8)$$

where K_{DCM} is static gain of the dc motor; T_{EM} is electromechanical constant of the dc motor.

The challenge in analysis of such systems is a mathematical representation of PWM block using transfer functions. This block is essentially a nonlinear component where gain depends on both frequency and input signal γ. Analysis of this block is usually based on various linearisation and assumptions that inevitably affect the accuracy of the results.

The low accuracy analysis of a sampled-data stabilising system can be conducted in a large signal mode where the duty cycle is changed over a wide range. If the system has a low cut-off frequency, a dc component of output signal of PWM converter is only used for analysis based on a saturation

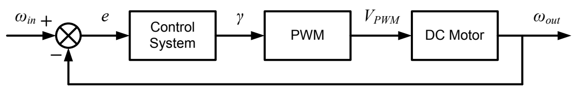

Fig. 2. Block diagram of sampled-data single-loop feedback system of speed stabilising

nonlinearity of the regulation characteristic of the convertor. The system can be linearised using a method of statistical linearisation in order to provide the transfer functions based further analysis. Denisov et al. (1995) shown that a sampled-data control system having the same type of nonlinearity can be analysed using Hermit polynomials approximation where weight function has a normal distribution of random variable (Marzocca et al., 2008).

However, analysis of broadband stabilising or high precision systems should involve the impact of variable component of PWM output signal on error. The output signal of PWM converter is a complex function depending on disturbance. Its general solution can be found using a multi-channel model based on approximation of PWM output signal by Walsh functions given below.

$$V_{PWM}(t,\gamma) = \sum_{k=0}^{\infty} a_k(\gamma)\, wal(k, t/T) \tag{9}$$

$$a_k(\gamma) = \frac{1}{T}\int_0^T V_{PWM}(t,\gamma)\, wal(k,t/T)\, dt \tag{10}$$

where T is the switching period.

Walsh functions are used as a basis for decomposition because of similarity of their waveform to the waveform of PWM output signal. However the decomposition of infinite series should be limited by a certain number of functions. Denisov et al., (1995) shown that the first 4 functions in decomposition ($wal0 = wal(0,t)$, $sal1 = wal(1,t)$, $cal1 = wal(2,t)$, $sal2 = wal(3,t)$) can provide accuracy of 95%.

Therefore, the system with deep PWM is an equivalent of the multi-channel model with a nonlinear pulse-amplitude modulation by Walsh functions. Fig. 3 shows the multi-channel model with an equivalent pulse-amplitude modulation, where K is gain of control system block where the output forms the duty cycle γ; S_0-S_3 are switching elements operating synchronously and in phase. NE_0-NE_3 are nonlinear elements in the channels. The amplitude variation patterns of Walsh functions during PWM have exactly the same shape as integrals of corresponding functions (Fig. 4, curves 1). This is why the amplitude characteristics of the nonlinear elements can be modelled at a high level of accuracy.

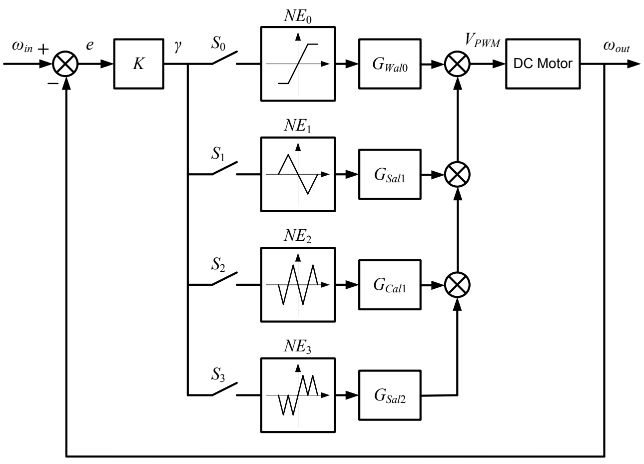

Fig. 3. Multi-channel model of stabilising system with an equivalent pulse-amplitude modulation.

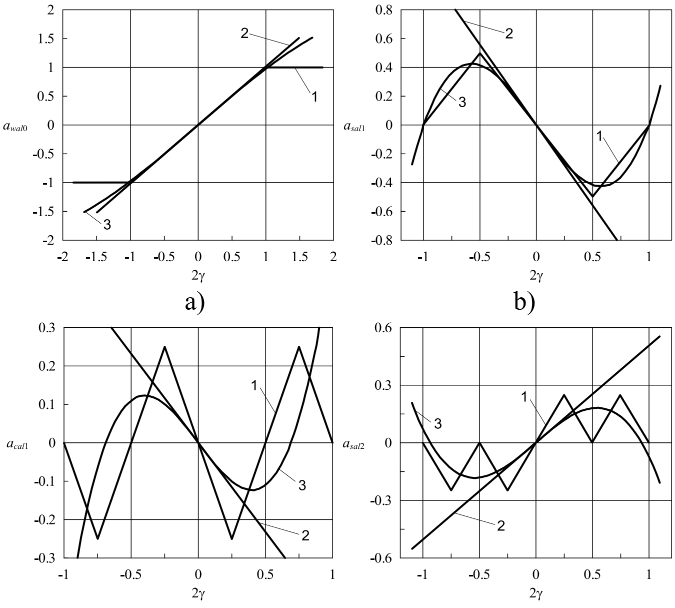

Fig. 4. The amplitude characteristics of channels of the converter model with a wide range of PWM: a) a_{Wal0} channel, b) a_{Sal0} channel, c) a_{Cal0} channel, d) a_{Sal0} channel.

The output signals of G-blocks described by the transfer functions G_{wal0} - G_{sal2} have the same waveform as Walsh functions $wal(0,t)$, $wal(1,t)$, $wal(2,t)$, $wal(3,t)$.

The level of nonlinearity of every channel depends on the range of error variation. Fig. 4 shows that the dc component of channel of the function $wal0$ has much wider linear zone comparing to the channels $cal1$ and $sal2$.

It can be seen in Fig. 4 that the amplitude characteristics of elements NE_0-NE_3 are piecewise linear. Hence, the system is analysed as linear within the linear zones. The change in parameters occurred during transient moves PWM duty cycle through the zones resulting a jumplike change of gain of elements NE_0-NE_3. In this case, the total solution is composited by sewing individual solutions obtained for each zone with initial conditions. However, this approach does not provide an analytical expression of the control error.

To obtain an analytical solution the nonlinear characteristics of each channel of the model (Fig. 3) should be approximated by Hermite polynomials (1).

$$a_{Wal}(\gamma) = c_0 H_0(\gamma) + c_1 H_1(\gamma) + c_2 H_2(\gamma) + \ldots \tag{11}$$

where the coefficients of Hermite series are calculated according to (5).

$$c_m = \frac{1}{\sqrt{2\pi}\sigma}\int_{-\infty}^{+\infty} e^{-\frac{\gamma^2}{2\sigma^2}} a_{Wal}(\gamma) H_m(\gamma)\, d\gamma \tag{12}$$

where $H_m(\gamma)$ is Hermite polynomial, s is dispersion, $a_{wal}(\gamma)$ is the amplitude characteristic of nonlinear element NE_0-NE_3.

Polynomial approximation of nonlinearity of each channel is limited by third order because a further increase in order makes error calculation very complicated. The original nonlinearity of the channels (Fig. 3) are described by odd functions, that is why the approximating polynomials have the following form

Table 1. Result of approximation for amplitude characteristics

function	σ = 1	σ = 1/3
$\varphi_{wal0}(\gamma)$	$0.924660\gamma - 0.080657\gamma^3$	$1.010596\gamma - 0.039887\gamma^3$
$\varphi_{sal1}(\gamma)$	$-0.193255\gamma + 0.036698\gamma^3$	$-1.110728\gamma + 1.125772\gamma^3$
$\varphi_{cal1}(\gamma)$	$0.032377\gamma - 0.005467\gamma^3$	$-0.461862\gamma + 0.966519\gamma^3$
$\varphi_{sal2}(\gamma)$	$0.090781\gamma - 0.017001\gamma^3$	$0.507208\gamma - 0.578059\gamma^3$

$$a_{Wal}(\gamma) \approx \phi_{Wal}(\gamma) = c_1\gamma + c_3\gamma^3 \tag{13}$$

Table 1 shows the results of approximation of amplitude characteristics (Fig. 4a-d, curves 1) for two values of dispersion. Approximated functions $\varphi_{wal0}(\gamma)$, $\varphi_{sal1}(\gamma)$, $\varphi_{cal1}(\gamma)$, $\varphi_{sal2}(\gamma)$ consist of two terms which are of the first and the cubic degrees. The amplitude characteristics of channels are straight lines (Fig. 4a-d, curves 2) if the approximated function is presented by the term of the first degree only. However, if the cubic term is additionally taken into account then the results of approximation are non-linear (Fig. 4a-d, curves 3).

Fig. 6 shows a model of the system with a wide range PWM where the amplitude characteristics of each channel are presented by both linear and nonlinear components. This is why every channel of the model is described by two discrete transfer functions - linear and nonlinear.

In order to simplify the analysis of system errors the following assumptions are accepted: (i) the dc motor is described as a first order element (8) and (ii) the control block is presented as a proportional element with gain K.

According to Schetzen (2006) the images of Volterra kernels for individual channels of system shown in Fig. 5 are composed using their transfer functions (14)-(21), where $q = sT$ is relative complex variable; $\alpha = T/T_{EM}$ is relative time constant

$$W_1^{Wal0}(q) = kc_1^{Wal0}\frac{1-e^{-q}}{q} \times \frac{\alpha}{q+\alpha} \tag{14}$$

$$W_1^{Sal1}(q) = kc_1^{Sal1}\frac{-1+2e^{-0.5q}-e^{-q}}{q} \times \frac{\alpha}{q+\alpha} \tag{15}$$

$$W_1^{Cal1}(q) = kc_1^{Cal1}\frac{-1+2e^{-0.25q}-2e^{-0.75q}+e^{-q}}{q} \times \frac{\alpha}{q+\alpha} \tag{16}$$

$$W_1^{Sal2}(q) = kc_1^{Sal2}\frac{1-2e^{-0.25q}+2e^{-0.5q}-2e^{-0.75q}+e^{-q}}{q} \times \frac{\alpha}{q+\alpha} \tag{17}$$

$$W_3^{Wal0}(q_1,q_2,q_3) = k^3c_3^{Wal0}\frac{1-e^{-(q_1+q_2+q_3)}}{q_1+q_2+q_3} \times \frac{\alpha}{q_1+q_2+q_3+\alpha} \tag{18}$$

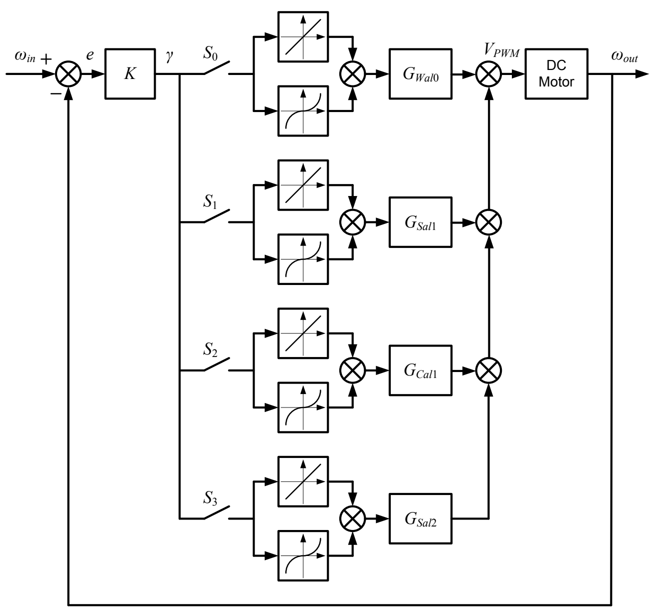

Fig. 5. Multi-channel model of system with a wide range PWM, taking into account the nonlinearities of elements.

of load; c_1^{wal}, c_1^{wal} are constant coefficients for γ and γ^3 in the expressions for approximated amplitude characteristics listed in Table 1; T is switching period; $k = K'K_{DCM}$.

A multidimensional discrete transfer function of each channel can be obtained using a multidimensional Z-transform (Rugh, 1981). The integral (22) is defined by sequential calculation of residues for all poles of multidimensional function $W_n^{Wal}(q_1,...,q_n)$.

$W_1^{Wal}(z,0)$ can be found as below.

$$W_1^{Wal}(z,0) = \left(\frac{1}{2\pi j}\right)\int_{c_1-j\infty}^{c_1+j\infty}\frac{1}{T}W_1^{Wal}(q)\frac{1}{1-e^{q}z^{-1}}dq \tag{23}$$

$$W_1^{Wal0}(z,0) = kc_1^{Wal0}\frac{1-e^{-\alpha}}{z-e^{-\alpha}} \tag{24}$$

$$W_1^{Sal1}(z,0) = kc_1^{Sal1}\frac{\left(e^{-0.5\alpha}-1\right)^2}{z-e^{-\alpha}} \tag{25}$$

$$W_1^{Cal1}(z,0) = kc_1^{Cal1}\frac{\left(e^{-0.5\alpha}-1\right)\left(e^{-0.25\alpha}-1\right)^2}{z-e^{-\alpha}} \tag{26}$$

$$W_1^{Sal2}(z,0) = kc_1^{Sal2}\frac{-\left(e^{-0.5\alpha}+1\right)\left(e^{-0.25\alpha}-1\right)^2}{z-e^{-\alpha}} \tag{27}$$

$$W_3^{Sal1}(q_1,q_2,q_3) = k^3c_3^{Sal1}\frac{-1+2e^{-0.5(q_1+q_2+q_3)}-e^{-(q_1+q_2+q_3)}}{q_1+q_2+q_3} \times \frac{\alpha}{q_1+q_2+q_3+\alpha} \tag{19}$$

$$W_3^{Cal1}(q_1,q_2,q_3) = k^3c_3^{Cal1}\frac{-1+2e^{-0.25(q_1+q_2+q_3)}-2e^{-0.75(q_1+q_2+q_3)}+e^{-(q_1+q_2+q_3)}}{q_1+q_2+q_3} \times \frac{\alpha}{q_1+q_2+q_3+\alpha} \tag{20}$$

$$W_3^{Sal2}(q_1,q_2,q_3) = k^3c_3^{Sal2}\frac{1-2e^{-0.25(q_1+q_2+q_3)}+2e^{-0.5(q_1+q_2+q_3)}-2e^{-0.75(q_1+q_2+q_3)}+e^{-(q_1+q_2+q_3)}}{q_1+q_2+q_3} \times \frac{\alpha}{q_1+q_2+q_3+\alpha} \tag{21}$$

$$W_n^{Wal}(z_1,...,z_n,0) = \left(\frac{1}{2\pi j}\right)^n\int_{c_n-j\infty}^{c_n+j\infty}....\int_{c_1-j\infty}^{c_1+j\infty}\frac{1}{T}W_n^{Wal}(q_1,...,q_n)\prod_{i=1}^{n}\frac{dq_i}{1-e^{q_i}z_i^{-1}} \tag{22}$$

Fig. 6. Transformed block diagrams of system with wide range PWM: (a) closed-loop system, (b) equivalent open-loop system.

$W_3^{Wal}(z_1,z_2,z_3,0)$ can be determined as following:

$$W_3^{Wal}(z_1,z_2,z_3)=$$
$$=\left(\frac{1}{2\pi j}\right)^3\int\limits_{c_3-j\infty}^{c_3+j\infty}\int\limits_{c_2-j\infty}^{c_2+j\infty}\int\limits_{c_1-j\infty}^{c_1+j\infty}\frac{1}{T}W_3^{Wal}(q_1,q_2,q_3)\frac{1}{1-e^{q_1}z_1^{-1}}\times \tag{28}$$
$$\times\frac{1}{1-e^{q_2}z_2^{-1}}\times\frac{1}{1-e^{q_3}z_3^{-1}}dq_1dq_2dq_3$$

$$W_3^{Wal0}(z_1,z_2,z_3,0)=k^3c_3^{Wal0}\frac{1-e^{-\alpha}}{z_1z_2z_3-e^{-\alpha}} \tag{29}$$

$$W_3^{Sal1}(z_1,z_2,z_3,0)=k^3c_3^{Sal1}\frac{\left(e^{-0.5\alpha}-1\right)^2}{z_1z_2z_3-e^{-\alpha}} \tag{30}$$

$$W_3^{Cal1}(z_1,z_2,z_3,0)=k^3c_3^{Cal1}\frac{\left(e^{-0.5\alpha}-1\right)\left(e^{-0.25\alpha}-1\right)^2}{z_1z_2z_3-e^{-\alpha}} \tag{31}$$

$$W_3^{Sal2}(z_1,z_2,z_3,0)=k^3c_3^{Sal2}\frac{-\left(e^{-0.5\alpha}+1\right)\left(e^{-0.25\alpha}-1\right)^2}{z_1z_2z_3-e^{-\alpha}} \tag{32}$$

The system shown in Fig. 5 can be transformed into the block diagram in Fig. 6a where linear and nonlinear discrete transfer functions are combined into separate units. The transfer functions in Fig. 6a are expressed as following.

$$W_1^{\Sigma}(z,0)=\sum_{i=0}^{3}W_1^{Wal_i}(z,0)=k\frac{k_1(\alpha)}{z-e^{-\alpha}} \tag{33}$$

$$W_3^{\Sigma}(z_1,z_2,z_3,0)=\sum_{i=0}^{3}W_3^{Wal_i}(z_1,z_2,z_3,0)=k^3\frac{k_3(\alpha)}{z_1z_2z_3-e^{-\alpha}} \tag{34}$$

The equivalent open-loop block diagram demonstrated in Fig. 6b is obtained according to Rugh (1981) to find error in closed system. Transfer functions of open-loop system for the first and the third components (Fig. 6b) can be found by the following expressions.

$$H_{e,1}(z,0)=\frac{1}{1+\Sigma W_1(z,0)} \tag{35}$$

$$H_{e,3}(z_1,z_2,z_3,0)=\frac{-\Sigma W_3(z_1,z_2,z_3,0)\prod_{i=1}^{3}H_{e,1}(z_i,0)}{1+\Sigma W_1(z_1z_2z_3,0)} \tag{36}$$

As mentioned previously, the response and the error of control consist of two components based on the first and the third approximations.

$$e[n]=e_1[n]+e_3[n] \tag{37}$$

$$\omega_{out}[n]=\omega_{out1}[n]+\omega_{out3}[n] \tag{38}$$

Assuming that the system input signal is a step function, the image of the first (linear) component of the error has the following form.

$$e_1(z,0)=H_{e,1}(z,0)G(z)=\frac{z\left(z-e^{-\alpha}\right)}{(z-L)(z-1)} \tag{39}$$

where $G(z)=\dfrac{z}{(z-1)}$ is the image of input influence; $L = e^{-\alpha} - kk_1(\alpha)$.

The image of third (nonlinear) component of the error is

$$e_3(z,0)=F_3\left[H_{e,3}(z_1,z_2,z_3,0)G(z)_1\,G(z_2)G(z_3)\right] \tag{40}$$

where F_3 is the operator of transition from three-dimensional to one-dimensional Z-transform.

The result can be obtained as

$$e_3(z_1,z_2,z_3,0)=k^3k_3(\alpha)\times$$
$$\times\frac{\left(z_1-e^{-\alpha}\right)\left(z_2-e^{-\alpha}\right)\left(z_3-e^{-\alpha}\right)z_1z_2z_3}{(z_1-L)(z_2-L)(z_3-L)(z_1z_2z_3-L)(z_1-1)(z_2-1)(z_3-1)} \tag{41}$$

To calculate the original of third component of the error the equation (47) should be converted using the theorem of transition of a single variable in complex plane (Schetzen, 2006).

$$Y(z)=F_k\left\{Y(z_1,...,z_k)\right\}=$$
$$=\frac{1}{(2\pi j)^{k-1}}\int\limits_{C_{k-1}}...\int\limits_{C_1}Y\left(z_1,...,z_{k-1},\frac{z}{\prod_{i=1}^{k-1}z_i}\right)\prod_{i=1}^{k-1}\frac{dz_i}{z_i} \tag{42}$$

$$e_3(z,0)=F_3\left\{e_3(z_1,z_2,z_3,0)\right\}=$$
$$=\frac{1}{(2\pi j)^2}\int\limits_{C_2}\int\limits_{C_1}e_3\left(z_1,z_2,\frac{z}{z_1z_2},0\right)\frac{dz_1}{z_1}\frac{dz_2}{z_2} \tag{43}$$

Finally

$$e_3(z,0)=k^3k_3(\alpha)\frac{z\left(z^3-Xz^2-Cz-V\right)}{\left(z-L^3\right)\left(z-L^2\right)(z-L)^2(z-1)} \tag{44}$$

where $X = 3L^2e^{-2\alpha} - 3Le^{-2\alpha} + 6Le^{-\alpha} + 3e^{-\alpha} + e^{-3\alpha} - 3e^{-2\alpha} - 2L^2 - 2L$; $C = 3L^3e^{-\alpha} - 3L^3e^{-2\alpha} + 2L^2e^{-3\alpha} - 6L^2e^{-2\alpha} - 3Le^{-2\alpha} + 3L^2e^{-\alpha} + 2Le^{-3\alpha} - L^3$; $V = L^3e^{-3\alpha}$.

The original error in terms of time domain can be found using the following equation (Rugh, 1981).

$$f[n]=Z^{-1}\left\{F(z)\right\}=$$
$$=\frac{1}{2\pi j}\int\limits_{L}F(z)z^{n-1}dz=\sum_{\nu}\underset{z_\nu}{\mathrm{Res}}\left[F(z)z^{n-1}\right] \tag{45}$$

$$\varepsilon_1[n]=Z^{-1}\left\{e_1(z,0)\right\}=\underset{\substack{z=L\\z=1}}{\mathrm{Res}}\frac{z^n\left(z-e^{-\alpha}\right)}{(z-L)(z-1)}=\frac{L^n\left(L-e^{-\alpha}\right)}{L-1}+\frac{1-e^{-\alpha}}{1-L}=\frac{1}{L-1}\left[L^n\left(L-e^{-\alpha}\right)-\left(1-e^{-\alpha}\right)\right] \tag{46}$$

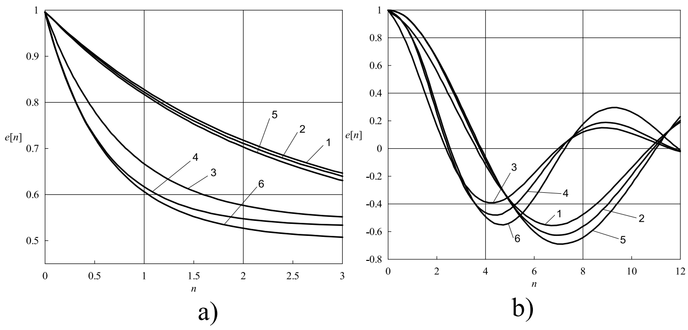

Fig. 7. Error of system control with wide range PWM for (a) proportional and (b) proportionally-integral regulators.

Therefore, the expression for first component of the error in time domain is obtained as (46). The expression (47) shows the third component of the error in time domain (Schetzen, 2006). Adding expressions (46) and (47) produces the error of system in general form which can be minimised by an adjusting the gain of the system. If the order of the system is higher than the first then the procedure to minimise the error can be performed by setting of parameters.

4. RESULTS AND DISCUSSION

In order to validate the analytical results the system was modelled and simulated using Matlab. Analysis was performed for two cases: (i) the amplitude characteristics of the channels (Fig. 4, curve 3) was approximated by Hermite polynomials; (ii) modelling and simulation was conducted using real amplitude characteristics of the channels (Fig. 4, curve 1).

The results for the first case have completely coincided with the analytical solution. However, the error modelled using the real amplitude characteristics of the channels (Fig. 4, curve 1) does not completely coincide with analytical results. Fig. 7 shows that the curves 5 ($\alpha = 0.2$) and 6 ($\alpha = 0.5$), which reflect actual non-linearity of channels, are different to the curves 2 and 4 obtained analytically. As can be seen the maximum difference between curves is quite small and does not exceed 10%.

The results of the error are presented in Fig. 7 where the curves 1 and 3 are related to the first approximation, and the curves 2 and 4 are related to the total approximation consisting of the first and the third. The curves 1 and 2 are corresponding to $\alpha = 0.2$; the curves 3 and 4 to $\alpha = 0.5$. It can be seen that the error is decreasing with increase in α as inertia of the system is reduced. In this case the difference between the curves of the first and the total approximations is increased that indicates the growing role of the third approximation under the rise of the cut-off frequency of the system.

5. CONCLUSIONS

The paper presents a new method of analysis of systems with a wide range PWM which based on the proposed model of converter using multidimensional discrete Laplace transform and Volterra series. In general the method assesses the impact of the system parameters on the quality of transients and provides adjustment of the regulator parameters to the optimum.

It has been shown that the inclusion of the third coefficient in Hermite approximation of the nonlinear amplitude characteristics of the multi-channel model improves the accuracy of the transient analysis comparing with the linearised model. A sampled-data stabilising system based on a dc electric drive has been used as an example to show that the impact of the third component of the approximation on the accuracy of the transient analysis is increased with the rise of the system bandwidth.

Using obtained analytical expression of an error the system can be optimised in order to achieve the minimum of the total error. This optimisation can be used in electric drives with precision stabilising system operating at a high accuracy.

REFERENCES

Burden, R.L. and Faires, J.D. (2011). *Numerical Analysis*. Boston, MA: BrooksCole, Cengage Learning.

Denisov, A.I., Zvolinsky, V.M. and Rudenko, Y.V. (1995). *Valve Converters in Precise Stabilization Systems*. Kiev: Naukova Dumka. (in Russian)

Lang, Z.Q, Billings, .S.A., Yue, R. and Li, J. (2007). Output frequency response function of nonlinear Volterra systems, *Automatica*, Vol. 43, No. 5, pp. 805-816.

Li, L.M. and Billings, S.A. (2011). Analysis of nonlinear oscillators using Volterra series in the frequency domain, *Journal of Sound and Vibration*, Vol. 330, No. 2, pp. 337 -355.

Marzocca, P., Nicholsb, J.M., Milanesea, A., Seaverb, M. and Trickeyb, S.T. (2008). Second-order spectra for quadratic nonlinear systems by Volterra functional series: Analytical description and numerical simulation, *Mechanical Systems and Signal Processing*, Vol. 22, No. 8, pp. 1882-1895.

Pavlov, A., Van de Wouw, N. and Nijmeijer, H. (2007). Frequency response functions for nonlinear convergent systems, *IEEE Transactions on Automatic Control*, Vol. 52, No. 6, pp. 1159-1165.

Rugh, W.J. (1981) *Nonlinear System Theory: The Volterra-Wiener Approach*. Baltimore: Johns Hopkins University Press.

Schetzen, M. (2006). *The Volterra and Wiener Theories of Nonlinear Systems*. Malabar, FL: Krieger Pubshing.

$$\varepsilon_3[n] = -k^3 d_3\left(1-e^{-\alpha}\right)\times\left(\frac{\left(L^3\right)^n\left(L^9-XL^6-CL^3-V\right)}{\left(L^3-L^2\right)\left(L^3-L\right)^2\left(L^3-1\right)}+\frac{\left(L^2\right)^n\left(L^6-XL^4-CL^2-V\right)}{\left(L^2-L^3\right)\left(L^2-L\right)^2\left(L^2-1\right)}+\frac{\left(1-X-C-V\right)}{\left(1-L^3\right)\left(1-L^2\right)\left(1-L\right)^2}\right)+ \\ +k^3 d_3 e^{-\alpha}\frac{L^n\left(An+S\right)}{L^3\left(L-1\right)^2\left(L-1\right)^4} \tag{47}$$

where $A = CLe^{\alpha} + L^3e^{\alpha} + L^4Xe^{\alpha} + V - Ve^{\alpha} + L^2Ve^{\alpha} + L^5 - L^5e^{\alpha} + + L^3Ce^{\alpha} - L^2Xe^{\alpha} + L^2X - L^3 - CL^3 - VL^2 - XL^4 - CL$;
$S = -L^2Ve^{\alpha} + L^3e^{\alpha} - 2L^5e^{\alpha} + 2Ve^{\alpha} - L^3 - 2V + VL^2 + CLe^{\alpha} + 2L^5 + + L^4Xe^{-3\alpha} - CL - VL^4$.